ISSN 0021-3640, JETP Letters, 2019, Vol. 110, No. 12, pp. 766–770. © Pleiades Publishing, Inc., 2019.
Russian Text © The Author(s), 2019, published in Pis'ma v Zhurnal Eksperimental'noi i Teoreticheskoi Fiziki, 2019, Vol. 110, No. 12, pp. 772–776.

OPTICS
AND LASER PHYSICS

Stimulated Raman Scattering in Metal–Dielectric Nanocomposites with Spectrally Degenerate Dielectric Constant

M. D. Tyugaev[a], A. V. Kharitonov[a], A. R. Gazizov[a, b], A. I. Fishman[a], M. Kh. Salakhov[a, b], A. A. Dedkova[c], A. M. Alekseev[a, c], A. V. Shelaev[a, d], and S. S. Kharintsev[a, b, *]

[a] *Institute of Physics, Kazan State University, Kazan, 420008 Russia*
[b] *Institute of Applied Research, Academy of Sciences of Tatarstan, Kazan, 420111 Russia*
[c] *National Research University of Electronic Technology (MIET), Zelenograd, Moscow, 124498 Russia*
[d] *OOO NT-MDT, Zelenograd, Moscow, 124460 Russia*
**e-mail: skharint@gmail.com*

Received October 28, 2019; revised November 9, 2019; accepted November 12, 2019

The effects of enhancement of stimulated Raman scattering in titanium oxynitride (TiON) nanofilms are considered. The mechanism of giant amplification of a Stokes wave is based on, first, localized plasmon resonance in titanium nitride (TiN) nanoparticles and, second, a spectrally degenerate behavior of the real part of the dielectric constant of the nanocomposite film. The enhancement of stimulated Raman scattering in the TiON film by means of a plasmonic nanoantenna and a nanostructured surface of the TiON film is demonstrated experimentally.

DOI: 10.1134/S0021364019240081

Stimulated Raman scattering (SRS) is a third order nonlinear optical effect when low-frequency vibrations of molecules can be coherently excited in a medium owing to the nonlinear interaction of the laser pump wave at the frequency ω_0 with the scattered Stokes wave at the frequency $\omega_s = \omega_0 - s\Omega$ (where Ω is the phonon frequency and $s = 1, 2, \ldots$; see Fig. 1b). Because of such four-wave mixing, the energy from the pump wave is transferred into the Stokes wave until their amplitudes become equal. In the continuous pump wave approximation ($I_0 \approx$ const), the intensity of the Stokes wave has the form [1]

$$I_s(L) = I_s(0)\exp[\chi_R I_0 L], \quad (1)$$

where L is the interaction length and χ_R is the enhancement factor of Raman scattering, which is defined as follows [1]:

$$\chi_R = -\frac{3\omega_s}{n_0 n_s \varepsilon_0 c^2}\mathrm{Im}[\chi^{(3)}]. \quad (2)$$

Here, $\chi^{(3)}$ is the cubic susceptibility of the medium, ε_0 is the permittivity of free space, c is the speed of light in the vacuum, and n_0 and n_s are the real refractive indices of the medium for the pump and Stokes waves (it is assumed that the medium is non-absorbing), respectively. For most natural materials, the inequalities $\chi^{(1)} \gg \chi^{(2)} \gg \chi^{(3)}$ are valid (e.g., $\chi^{(1)} \sim 1$, $\chi^{(2)} \sim 10^{-13}$–10^{-9} m/V, and $\chi^{(3)} \sim 10^{-23}$–10^{-18} m^2/V^2). This means that nonlinear effects are weak and their observation requires increasing the interaction length L (e.g., using optical fibers) and/or the laser pump power I_0 (using high-power pulsed lasers). As a result, it is impossible to generate SRS in spatially limited materials (nanostructures) or on single molecules illuminated by low-intensity laser light ($I_0 < 1$ MW/cm^2). However, coherent anti-Stokes Raman scattering (CARS) [2] and SRS [3] were experimentally observed by placing a single molecule near a metallic (plasmonic) nanoantenna or in a 3D nanocavity. Enhancement of nonlinear optical effects is due to giant local electric fields and changes in the properties of the radiating/absorbing system (see Fig. 1a).

In the approximation $\omega_0 \approx \omega_s$, the local enhancement factor of Raman scattering can be represented as

$$G(\mathbf{r}, \omega) \simeq g_0^4(\mathbf{r}, \omega) g_1^4(\mathbf{r}, \omega) g_2^4(\mathbf{r}, \omega). \quad (3)$$

The fourth power indicates that the effect of laser light localization on the enhancement of nonlinear optical effects is described by the product of the average local enhancement factors of the optical fields involved in light scattering. The first factor corresponds to the local enhancement of the optical field due to the action of the nanoantenna (green arrows in Fig. 1a) and is defined as

$$g_0(\mathbf{r}, \omega) = \frac{|\mathbf{E}(\mathbf{r}, \omega)|}{|\mathbf{E}_0(\mathbf{r}, \omega)|}, \quad (4)$$

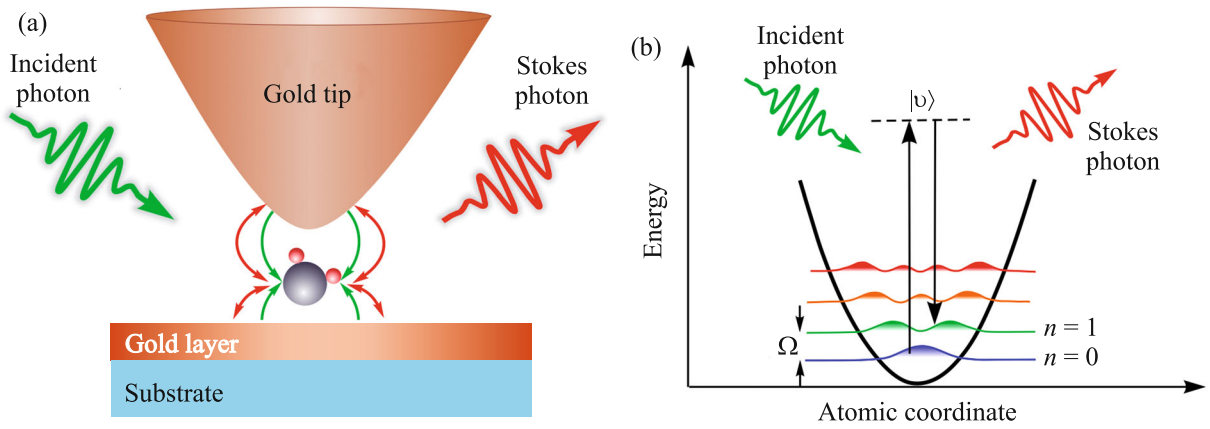

Fig. 1. (Color online) (a) Diagram of the interaction of a molecule with a locally enhanced optical field created by a plasmonic nanoantenna and a metal substrate. (b) Energy diagram for the demonstration of Raman scattering; the parabola indicates the absence of anharmonicity.

where $\mathbf{E}_0(\mathbf{r},\omega)$ and $\mathbf{E}(\mathbf{r},\omega)$ are the intensities of the incident and amplified optical fields at the point $\mathbf{r}$, respectively, and ω is the frequency of the incident wave. The second multiplier describes the effect of multiple self-action of the scattered optical field (red arrows in Fig. 1a) per molecule and has the form [4]

$$g_1(\mathbf{r},\omega) \simeq 1/3\mathrm{Tr}\{[\ddot{\mathbf{I}} - \beta\ddot{\mathbf{G}}_s(\mathbf{r},\mathbf{r},\omega)]^{-1}\}, \quad (5)$$

where Tr{...} denotes the trace of the matrix, $\ddot{\mathbf{I}}$ is the identity matrix, β is the polarizability of the molecule, and $\ddot{\mathbf{G}}_s(\mathbf{r},\mathbf{r},\omega)$ is the dyadic Green's function for multiple scattering. The third multiplier $g_2(\mathbf{r},\omega)$ is responsible for the resonant exchange interaction between the vibrational mode of the molecule and the optical mode of the nanocavity and corresponds to the strong coupling mode [5]. This contribution allows the generation of SRS from a single molecule.

In our work, a 50-nm titanium nitride (TiN) film was chosen as a spatially limited nonlinear medium, for which the cubic nonlinearity can reach $\chi^{(3)} = -(5.3 + 0.2i)\times10^{-18}$ m^2/V^2 [6]. The film was synthesized on a SiO_2/Si substrate by magnetron sputtering in an Ar : N_2 (50 : 50) atmosphere at a temperature of 350°C. Oxidation of the film in air leads to the formation of crystalline and amorphous TiO_xN_y phases. Figure 2a shows an atomic force microscopy image of the film surface. As shown in [7, 8], the chemical structure of the film can be approximated as a binary mixture of TiN metal nanoparticles and dielectric nanoparticles (TiO_2): TiON = fTiN + $(1-f)TiO_2$ (where f is the volume filling factor, $0 < f < 1$). Figure 2b shows a log-scale map of the conductivity of the TiON film, which shows a percolation behavior: the bright regions correspond to the presence of continuous conducting chains in the medium. A unique property of such a nanocomposite film is an unusual behavior of the real part of the dielectric constant of TiON, which twice becomes zero in the visible and near-infrared regions at the epsilon-near-zero (ENZ) frequencies, as shown in Fig. 2c. As seen in Fig. 2c, the TiN film exhibits a metallic behavior with large optical losses (the imaginary part of the dielectric constant) compared to TiON.

The effective cubic nonlinear susceptibility of metal–dielectric nanocomposite films can be represented by averaging the contributions from metal and dielectric inclusions [9]:

$$\chi^{(3)}_{\mathrm{eff}} = f\hat{g}_0^2\hat{g}_k^2\chi^{(3)}_{\mathrm{m}} + (1-f)\hat{G}_0^2\hat{G}_k^2\chi^{(3)}_{\mathrm{d}}. \quad (6)$$

Here, $\chi^{(3)}_{\mathrm{m}}$ and $\chi^{(3)}_{\mathrm{d}}$ are the cubic nonlinearities for TiN and TiO_2, respectively; $\hat{g}_i = \hat{g}(\omega_i)$ and $\hat{G}_i = \hat{G}(\omega_i)$ $(i = (0, s))$ are the complex local enhancement factors of the optical field given by the formulas

$$\hat{g}(\omega) = \frac{\varepsilon_{\mathrm{eff}}(\omega) + 2\varepsilon_{\mathrm{d}}(\omega)}{\varepsilon_{\mathrm{m}}(\omega) + 2\varepsilon_{\mathrm{d}}(\omega)},$$
$$\hat{G}(\omega) = \frac{\varepsilon_{\mathrm{eff}}(\omega) + 2\varepsilon_{\mathrm{d}}(\omega)}{3\varepsilon_{\mathrm{d}}(\omega)}, \quad (7)$$

where $\varepsilon_{\mathrm{eff}}(\omega)$ is the effective dielectric constant of the nanocomposite, which can be found from the theory of the effective medium [10]. Since $\varepsilon_{\mathrm{eff}}(\omega) \to 0$ ($\varepsilon_{\mathrm{eff}} = \varepsilon'_{\mathrm{eff}} + i\varepsilon''_{\mathrm{eff}}$, where $\varepsilon'_{\mathrm{eff}}$ and $\varepsilon''_{\mathrm{eff}}$ are the real and imaginary parts of the dielectric constant, respectively), $\hat{G}(\omega) \approx 1$ and, thus, the plasmon contribution $\hat{g}(\omega)$ becomes dominant in the nonlinear enhancement of the optical signal. On the other hand, when $\varepsilon'_{\mathrm{eff}} \approx 0$, the real n'_k and n''_k imaginary parts of the refractive index of the medium for the Stokes wave satisfy the relation $n'_k \simeq n''_k = \sqrt{\varepsilon''_{\mathrm{eff}}/2}$. Thus, an additional

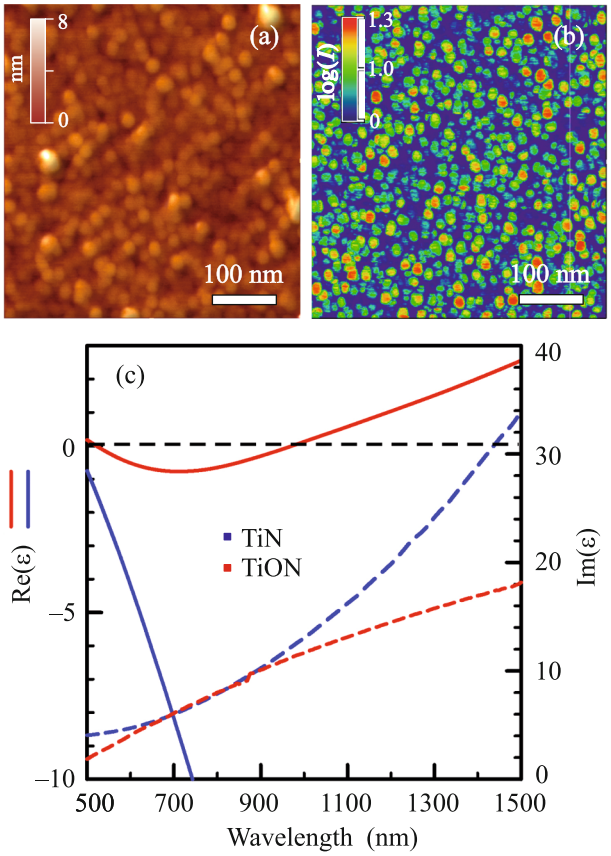

Fig. 2. (Color online) (a) Atomic force microscopy topography of a 50-nm TiON film. (b) Conductivity map of the TiON film on a logarithmic scale. (c) Real and imaginary parts of the dielectric constants of TiN and TiON.

mechanism for nonlinear enhancement of the optical field appears at the ENZ frequencies [9]:

$$\chi_R(\omega_k) = -\frac{3\omega_m}{n_0\varepsilon_0 c^2}\,\mathrm{Im}\left[\frac{\chi^{(3)}_{\mathrm{eff}}}{n_k}\right] = \frac{3\omega_k}{n_0\varepsilon_0 c^2} \times \frac{\varepsilon''_{\mathrm{eff}}{}^{(3)} n''_k - \chi''_{\mathrm{eff}}{}^{(3)} n'_k}{n'_k{}^2 + n''_k{}^2} \simeq \frac{3\omega_k}{n_0\varepsilon_0 c^2}\,\frac{\chi'_{\mathrm{eff}}{}^{(3)} - \chi''_{\mathrm{eff}}{}^{(3)}}{\sqrt{2\varepsilon''_{\mathrm{eff}}}}. \quad (8)$$

This means that the creation of a nanocomposite with vanishingly small optical losses $\varepsilon''_{\mathrm{eff}} \to 0$ will lead to an amplification of the Stokes wave. Unlike Eq. (2), SRS is determined by both the imaginary and real components of the cubic nonlinearity $\chi^{(3)}$. The latter is responsible for changing the phase of the Stokes wave and, as a result, there is a nonlinear contribution to the refractive index of the medium (analogous to the Kerr effect).

Figure 3a shows the Raman spectra from a 50-nm TiON film with and without plasmonic (gold) nanoantenna. The Raman spectrum (blue line) indicates the appearance of a wide band in the region of 600–700 cm^{-1}, which belongs to the polymorphic modifications of TiO_2. The tip-enhanced Raman scattering (TERS) spectroscopy (red line) allowed resolving strongly overlapped spectral components and attributing them to rutile (600 and 630 cm^{-1}) and anatase (655 and 680 cm^{-1}) [8]. Thus, spectroscopic data confirm the binary structure of the TiON film [7].

An important observation is the appearance of the 480 cm^{-1} line, which can be attributed to the SRS line,

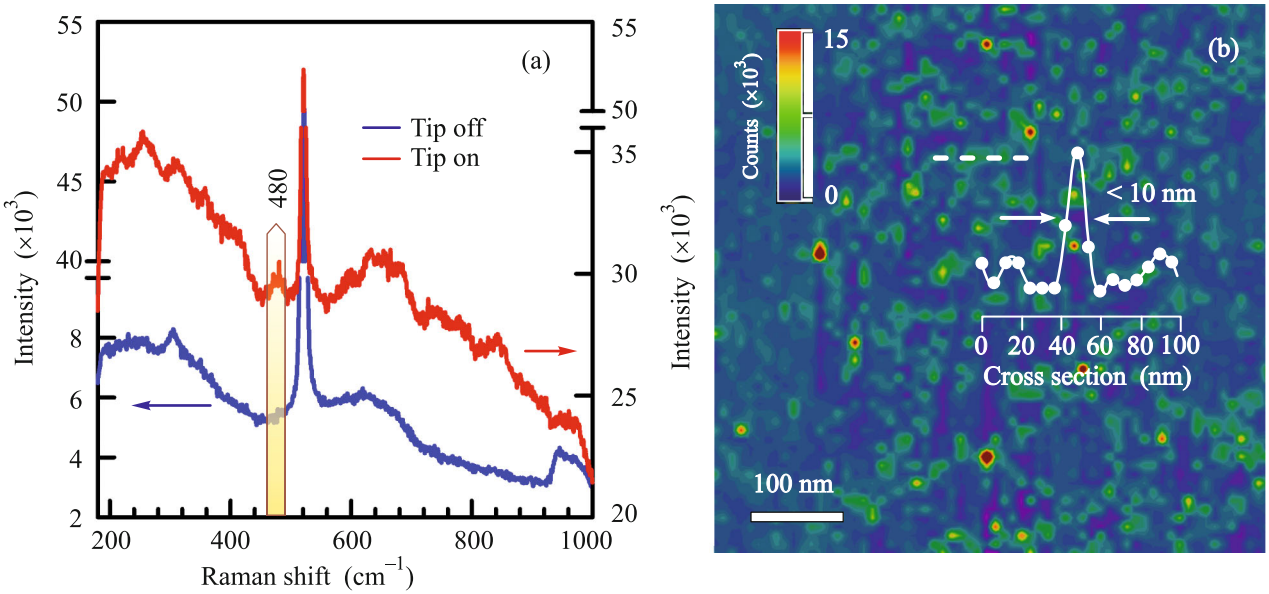

Fig. 3. (Color online) (a) Raman spectra of a 50-nm TiON film with and without the plasmonic antenna. (b) Map of TERS from a 50-nm TiON film.

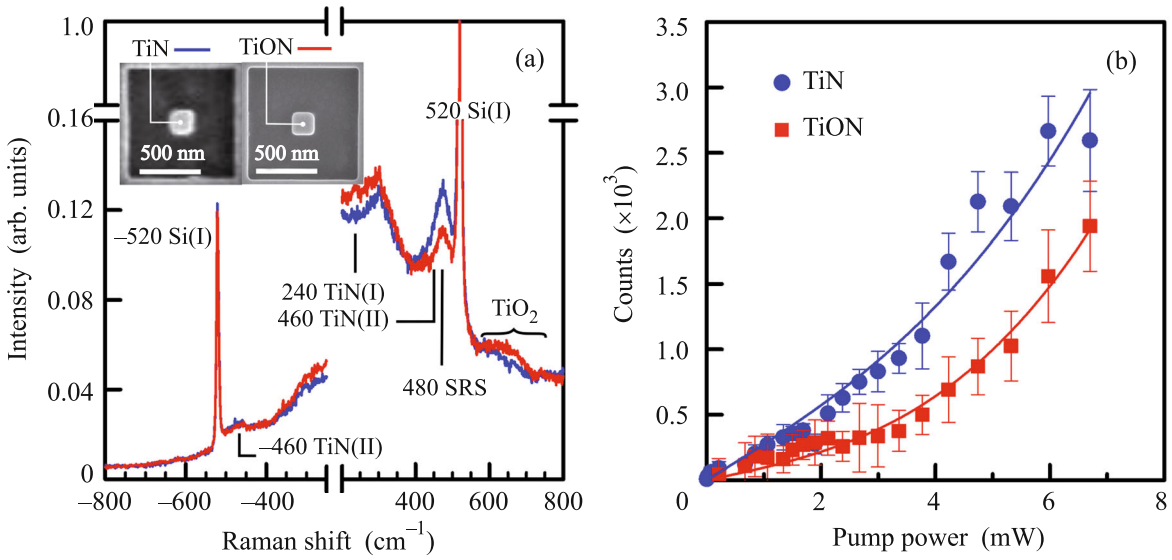

Fig. 4. (Color online) (a) Raman spectra from 200 × 200 nm square nanoantennas created using an ion beam on (blue line) TiN and (red line) TiON films 50 nm thick. The inset shows scanning electron microscopy images of the nanoantennas. (b) Intensity of the Stokes wave versus the intensity of incident light.

since the second TiN overtone is observed near 460 cm^{-1}. In [11], this effect was first observed on a 500 × 500-nm square nanoantenna. The appearance of the SRS effect on the TiON film in the presence of an optical nanoantenna can be explained by the enhanced cubic nonlinearity caused by the excitation of the plasmon gap mode. Figure 3b shows the TERS map for the TiON film. This map correlates with the results for the conductivity (see Fig. 2b). On both maps, the TiN nanoparticle sizes are estimated in the range of 10–20 nm. In particular, the TERS map allows a high spatial resolution better than 10 nm.

Figure 4a shows the Raman spectra from 200 × 200-nm square nanoantennas for (blue line) TiN and (red line) TiON, which were cut by a focused ion beam on the corresponding films. Scanning electron microscopy images of the antennas are shown in the inset of Fig. 4a. The Raman spectra from TiON also show a wide band in the region of 600–700 cm^{-1}, which allows the unambiguous identification of the source material. Owing to the nanostructuring of the film, it is possible to observe the SRS band at 480 cm^{-1} without using the TERS method. In this case, the analyzed structure itself acts as an amplifying antenna. One of the signatures of SRS is the absence of the anti-Stokes bands. In Fig. 4a, only the second TiN overtone at –460 cm^{-1} is observed in the anti-Stokes region. In contrast to TiN, the intensity of the SRS band at 480 cm^{-1} for TiON decreases because of a smaller number of TiN metal nanoparticles. The usual feature of SRS is the nonlinear dependence of the Stokes wave intensity on the pump wave intensity (see Fig. 4b). For clarity, these experimental data were approximated by the function

$$I_k \equiv I(\omega_k) \sim \sigma_1 I_p + \sigma_3 I_p^3, \quad (9)$$

where σ_1 and σ_2 are the coefficients proportional to the cross sections for spontaneous and induced light scattering. This separation is conditional and depends on the sensitivity of the recording system.

The cross sections for spontaneous Raman scattering for the two samples are 271 (TiN) and 91 (TiON), whereas the cross sections for SRS are 3.79 (TiN) and 4.32 (TiON). This means that, despite a smaller number of nonlinear oscillators in TiON, the observed enhancement exceeds the nonlinear contribution for TiN. This effect can be explained by the appearance of the Anderson localization in the metal–dielectric medium, which acts as an additional optical pump. This hypothesis requires additional theoretical and experimental research.

In conclusion, we note that the experimentally observed effects of SRS in titanium oxynitride (TiON) nanofilms is due to the strengthening of the effective cubic nonlinearity of the medium by means of the mechanism of excitation of localized plasmon resonances in titanium nitride (TiN) nanoparticles and the quasi-zero refractive index of the effective medium for the Stokes wave. Nanocomposite metal–dielectric films having several ENZ frequencies in the visible and infrared regions are applied to create broadband metalenses that provide subdiffraction resolution [8], as well as high-efficiency broadband solar light absorbers for thermophotovoltaics.

ACKNOWLEDGMENTS

We are grateful to the Ostec Group and ScanSens companies for technical support.

FUNDING

This work was supported by the Russian Science Foundation (project no. 19-12-00066).

REFERENCES

1. R. W. Boyd, *Nonlinear Optics* (Academic, San Diego, 2008).
2. S. Yampolsky, D. A. Fishman, S. Dey, E. Hulkko, M. Banik, E. O. Potma, and V. A. Apkarian, Nat. Photon. **8**, 650 (2014).
3. R. Zhang, Y. Zhang, Z. C. Dong, S. Jiang, C. Zhang, L. G. Chen, L. Zhang, Y. Liao, J. Aizpurua, Y. Luo, J. L. Yang, and J. G. Hou, Nat. Nanotechnol. **498**, 82 (2013).
4. C. Zhang, B. Q. Chen, and Z. Y. Li, J. Phys. Chem. C **119**, 11858 (2015).
5. M. K. Schmidt, R. Esteban, A. González-Tudela, G. Giedke, and J. Aizpurua, ACS Nano **10**, 6291 (2016).
6. N. Kinsey, A. A. Syed, D. Courtwright, C. DeVault, C. E. Bonner, V. I. Gavrilenko, V. M. Shalaev, D. J. Hagan, E. W. van Stryland, and A. Boltasseva, Opt. Mater. Express **5**, 2395 (2015).
7. L. Braic, N. Vasilantonakis, A. Mihai, I. J. V. Garcia, S. Fearn, B. Zou, N. McN. Alford, B. Doiron, R. F. Oulton, S. A. Maier, A. V. Zayats, and P. K. Petrov, ACS Appl. Mater. Interfaces **9**, 29857 (2017).
8. S. S. Kharintsev, A. V. Kharitonov, A. M. Alekseev, and S. G. Kazarian, Nanoscale **11**, 7710 (2019).
9. S. S. Kharintsev, Opt. Lett. **44**, 5909 (2019).
10. V. Shalaev and W. Cai, *Optical Metamaterials: Fundamentals and Applications* (Springer Science, New York, 2009).
11. S. S. Kharintsev, A. V. Kharitonov, S. K. Saikin, A. M. Alekseev, and S. G. Kazarian, Nano Lett. **17**, 5533 (2017).

Translated by V. Alekseev